

Novel configurations for the fabrication of high quality REBCO bulk superconductors by a modified RE + 011 top-seeded infiltration and growth process

Pengtao Yang^{ID}, Wanmin Yang, Lijuan Zhang and Li Chen

College of Physics and Information Technology, Shaanxi Normal University, Xi'an 710062, People's Republic of China

E-mail: yangwm@snnu.edu.cn

Received 14 March 2018, revised 30 May 2018

Accepted for publication 12 June 2018

Published 5 July 2018



Abstract

Single domain REBCO bulk superconductors can be fabricated by the top-seeded infiltration and growth (TSIG) process, but there are some problems with removing the residual liquid phase from the bulks after crystal growth. The superconducting bulks fabricated by the TSIG process are generally obtained by slicing or polishing the REBCO bulks, which may produce cracks in the samples. In order to solve these problems, we proposed two novel configurations to prevent the REBCO bulks fusing together with the residual liquid phase by introducing transport layers or bars between the solid phase pellets and the liquid phase pellets. It is found that the REBCO bulks fabricated by the RE + 011 TSIG process can be easily separated from the residual liquid phase by using new configurations. We have also fabricated GdBCO bulks with 1 wt% CeO₂ addition using the novel configuration. The CeO₂ doping GdBCO bulk with diameter of 20 mm exhibits a very good trapped field of 1.110 T and levitation force of 54.5 N at 77 K. The results indicate that this is not only a good way to fabricate high quality single domain REBCO bulks, but also an important way to fabricate near net shape REBCO bulks without any mechanical process.

Keywords: novel configurations, REBCO bulk superconductors, RE + 011 TSIG process, CeO₂ doping, trapped field

(Some figures may appear in colour only in the online journal)

1. Introduction

Single domain RE-Ba-Cu-O (REBCO, where RE is a rare earth element, such as Y, Gd, Nd, Sm, etc) bulk superconductors have a significant potential for use in various applications, such as magnetic bearings, magnetic separators, motors, flywheels, portable magnetic resonance imaging, energy storage systems, self-limiting transformer and levitated transportation systems [1–7] because of their strong pinning flux energy, high critical temperature and good self-stable levitation performance. The top-seeded infiltration and growth (TSIG) process has been widely used to fabricate REBCO bulk superconductors due to its prominent

advantages [8, 9]. But the traditional TSIG method is relatively more complicated and time consuming because it needs three kinds of precursor powders, such as REBa₂Cu₃O_y (RE-123), RE₂BaCuO₅ (RE-211) and Ba₃Cu₅O₈ (035). In order to improve the working efficiency and reduce the fabrication cost of the TSIG technique, the RE + 011 TSIG method with the solid phase of RE₂O₃ + 1.2BaCuO₂ and the liquid phase of Y₂O₃ + 10BaCuO₂ + 6CuO has been developed recently [10–13], with which it is only necessary to fabricate the powder of BaCuO₂ (011) in the laboratory.

The generic configuration illustration before growth and the surface morphologies of REBCO bulk superconductors fabricated by the RE + 011 TSIG process are shown in

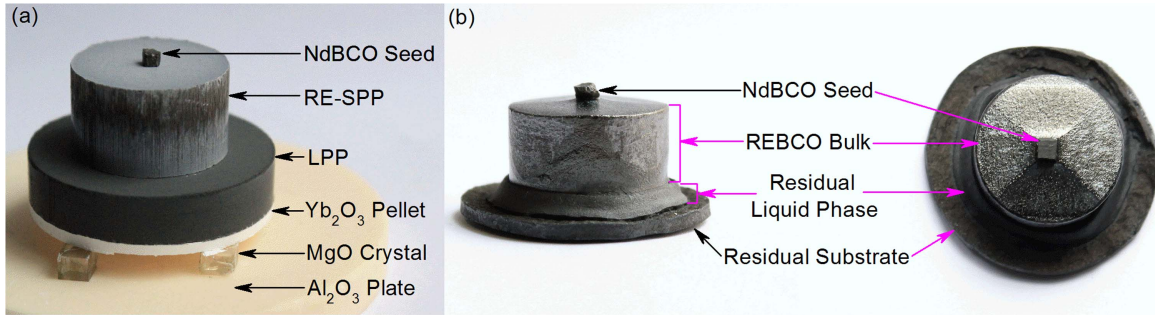


Figure 1. (a) The generic configuration illustrations of the REBCO samples before infiltration and growth. (b) The top and side surface morphologies of REBCO bulk superconductors fabricated by using the generic configuration in the RE + 011 TSIG process.

figure 1 [11, 12]. As we can see from figure 1, there are four parts in the as-grown sample, the NdBCO seed, the single domain REBCO bulk superconductor, the residual liquid phase and the residual substrate, but only the single domain REBCO bulk is useful for applications. The single domain REBCO bulk can be used effectively after it is cut off from the residual liquid phase or the residual substrate, which are eventually turned into waste after the TSIG process. Previous studies on Y-Ba-Cu-O (YBCO) bulk superconductors fabricated by a Y + 011 TSIG process indicate that high quality single domain YBCO bulks without any residual liquid phase can be fabricated by using a new liquid phase of 3BaCuO₂ + 2CuO to replace the liquid phase of Y₂O₃ + 10BaCuO₂ + 6CuO [13]. But the residual Yb₂O₃ substrates also need to be cut off from the YBCO bulks. So it is necessary to develop new methods to obtain the single domain REBCO bulk superconductors with an easily removable residual liquid phase in the TSIG process.

In addition, chemical doping has been proven to be an effective method to enhance the flux pinning force and physical properties of the REBCO superconductor, such as Pt and CeO₂ doping, which can refine the size of RE-211 particles and enhance the trapped field and J_c of the single domain REBCO superconductors. Kim *et al* [14, 15] reported that needle-like and highly anisotropic Y-211 particles which formed in single grain YBCO samples with CeO₂ doping contained finer Y-211 particles compared with Pt doping. Furthermore, Muralidhar *et al* [16, 17] extended the study into the (Nd, Eu, Gd)-BCO system and reported that a combined addition of Pt and CeO₂ is effective in reducing the size of the secondary-phase particles. Zhai *et al* [18] reported that YBCO bulk superconductors containing a graded-CeO₂ composition with diameters of 25 mm and 31 mm exhibited an enhanced trapped field of 0.81 T and 0.92 T at 77 K. Recently, Zhao *et al* [19] also clearly observed that addition of CeO₂ addition is significantly more effective and cheaper compared to addition of Pt in refining the secondary Sm-211 phase inclusions in the sample by the top-seeded melt texture growth (TSMG) method. More recently, a new RE + 011 TSIG method has been developed for the fabrication of high quality REBCO bulk superconductors, through which the levitation force of a single domain YBCO sample (20 mm in diameter) has reached about 50 N (77 K, 0.5 T), [10]. In this new method it is easy to refine the Y-211 particles to a finer

size (the average size is about 1 μm) in the samples without any Pt or CeO₂ additions. But this method is not so good for the single domain GdBCO samples, because the levitation force of the single domain GdBCO samples (20 mm in diameter) is about 28 N (77 K, 0.5 T), which is closely related to the larger Gd-211 particles (their average size is larger than 10 μm) in the samples [20]. In order to further improve the physical properties of single domain GdBCO samples, the larger size of Gd-211 particles has to be refined. Therefore it is important to investigate the effect of CeO₂ doping on the single domain GdBCO bulk superconductors fabricated by the RE + 011 TSIG process.

In this paper, we reported on the two novel configuration techniques for fabrication of single domain REBCO bulk superconductors with easily removable residual liquid phases in the TSIG process, and the fabrication of high quality GdBCO bulk superconductors by a combination of the novel configuration and CeO₂ doping.

2. Experimental details

Commercial powders of BaCO₃ and CuO at 99.0% purity, Gd₂O₃, Y₂O₃ and Yb₂O₃ at 99.9% purity and CeO₂ at 99.95% purity were used as precursor powders. The BaCuO₂ powder was made through the traditional solid state reaction by mixing BaCO₃ and CuO powders at a molar ratio of BaCO₃: CuO = 1:1. The mixture of BaCO₃ and CuO powders was ball-milled for 5 h and sintered at 900 °C for 24 h, and the process was repeated three times. Undoped solid phase compositions of Y₂O₃ + 1.2BaCuO₂ powder and Gd₂O₃ + 1.2BaCuO₂ powder were uniaxially pressed into a Y-solid phase pellet (Y-SPP) and a Gd-solid phase pellet (Gd-SPP) respectively using a steel mold 20 mm in diameter, the CeO₂ doped solid phase compositions of 99 wt% (Gd₂O₃ + 1.2BaCuO₂) + 1 wt% CeO₂ powder were also pressed into a pellet 20 mm in diameter. The liquid phase pellet (LPP) of Y₂O₃ + 10BaCuO₂ + 6CuO powder and the support substrate of Yb₂O₃ powder were uniaxially pressed into pellets together using a steel mold 32 mm in diameter.

For the first configuration technique, the transport layers containing Y₂O₃ + 1.2BaCuO₂ were prepared for the purposes of transporting the liquid phase to the Y-SPP, and at the same time, separating the Y-SPP and the residual liquid phase

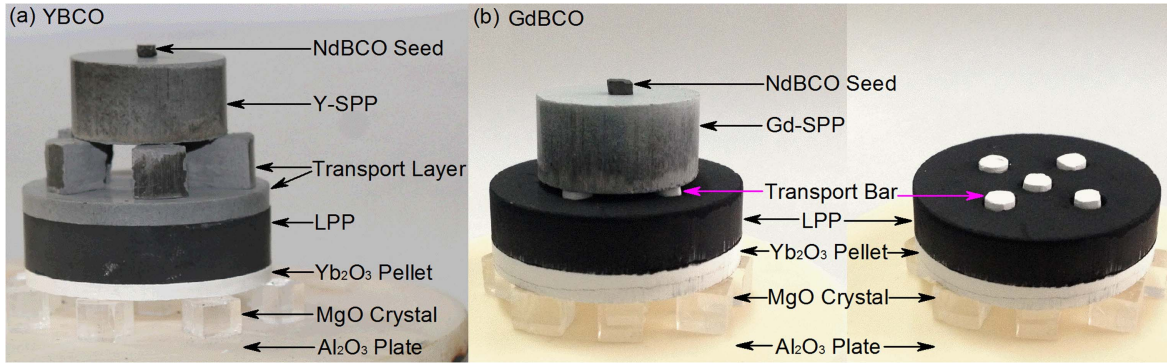


Figure 2. The novel configuration illustrations of the (a) YBCO and (b) GdBCO samples before RE + 011 TSIG process used in this study.

during infiltration and growth. The precursor sample was assembled with the three pressed pellets (Y-SPP, transport layers, LPP and Yb_2O_3 support substrate) and layered up together along their coaxial line, which were laid over several MgO crystals, and then an NdBCO crystal seed was placed at the top center of the SPP with the a–b plane parallel to the surface. The whole configuration is shown in figure 2(a). For the second configuration technique, the transport bars made of Y_2O_3 were inserted into the LPP to transport the liquid phase to the Gd-SPP, and at the same time, to separate the Gd-SPP and the residual liquid phase during infiltration and growth. The whole configuration is shown in figure 2(b). In addition, the GdBCO sample containing 1 wt% CeO_2 was also assembled by the second configuration method in the RE + 011 TSIG process.

Then the samples were put into a self-designed high-temperature furnace with an appropriate temperature gradient, which can effectively prevent the random nucleation of REBCO grains at the edges of the samples [12, 21, 22]. The heating profile of YBCO and GdBCO samples is shown in figure 3. Initially, YBCO samples were heated up to 900 °C at a rate of 150 °C h⁻¹ and this was followed by a 10 h dwelling for sintering to achieve the Y-211 phase, then further heating to 1045 °C in 1 h and holding for 1.5 h to ensure the complete infiltration of the liquid phase into the Y-SPP. After that, the samples were then quickly cooled to 1008 °C at a rate of 60 °C h⁻¹ and then were cooled slowly to 990 °C at a rate of 0.3 °C h⁻¹. Compared to the YBCO, Gd-123 has a higher melting temperature and peritectic reaction temperature, which should be first heated to 900 °C at a rate of 150 °C h⁻¹, followed by a 10 h dwelling for sintering to achieve the Gd-211 phase, and then heated to 1061 °C in 1 h and held for 1.5 h, after that, it should be cooled to 1031 °C rapidly and followed with a slower cooling to 1014 °C by 0.4 °C h⁻¹. Finally, the furnace was cooled to room temperature for both YBCO and GdBCO samples. The as-grown YBCO samples were oxygenated at 440 °C for 200 h and the GdBCO samples were heated up to 430 °C and then slowly cooled to 350 °C for 200 h under flowing pure oxygen respectively, so that the as-grown samples could complete the phase transition from a tetragonal phase to an orthorhombic phase and become superconducting materials.

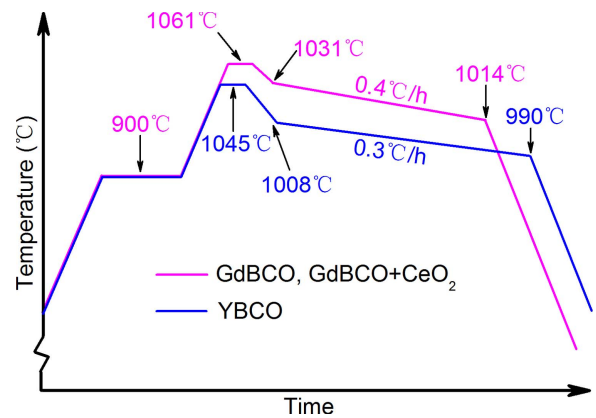


Figure 3. Heating profile used to fabricate single domain YBCO and GdBCO samples in the RE + 011 TSIG process.

In addition, the levitation forces and trapped fields were measured by using the self-designed 3D magnetic measurement system [23] and the microstructure of the samples was studied using a scanning electron microscope (SEM).

3. Results and discussion

3.1. Surface morphology

Figure 4 shows the surface morphologies of the YBCO and GdBCO bulk superconductors fabricated using the two novel configurations. We can see from figures 4(a) and (d) that there is a gap between the single grain REBCO bulk and the residual liquid phase or the substrate after infiltration and crystal growth, which is due to the separation of the transport layers and bars between the SPP and LPP. Figures 4(b) and (e) show the top views of the two samples. As can be seen, four-fold growth sectors initiated from the seed have spread over the whole top surface indicating that the samples are of single domain character, which means that the transport layers and bars can effectively transfer the liquid phase from the LPP to SPP and guarantee the successful growth of the single domain REBCO bulks. Figures 4(c) and (f) show the residual liquid phase and the final REBCO bulk superconductors after they were separated. We can obtain the final REBCO bulks without any residual liquid phase from the whole as-grown samples very easily by hand. This is the advantage of the



Figure 4. The surface morphologies of YBCO and GdBCO bulk superconductors fabricated using the novel configurations. (a), (d) Side view, (b), (e) top view, (c), (f) residual liquid phase and final REBCO bulk superconductors.

novel configurations, whose transport layers or bars can not only prevent the single domain REBCO bulk from fusing together with the residual liquid phase or the substrate, but also can provide a channel for supplying the liquid phase upward to promote the REBCO crystal growth continuously. Nearly net shape single domain REBCO bulk superconductors can be fabricated without any mechanical processes by these novel configuration techniques. Compared with the samples fabricated by the traditional TSIG process, in which the residual liquid phase or the substrate has to be removed by mechanical slicing or polishing after crystal growth, the novel configuration techniques may reduce the damage to the single domain REBCO bulk superconductors. Several REBCO bulks 20 mm in diameter and 8 mm in thickness were obtained by this new method. In addition, a single domain GdBCO bulk superconductor containing 1 wt% CeO₂ (GdBCO + CeO₂) was also fabricated successfully by the novel configuration method, which proves the feasibility of the novel configurations.

3.2. Levitation force

Figure 5 shows the levitation force–distance curves between the permanent magnet (NdFeB, $\Phi = 20$ mm, $B_{\text{pm}} = 0.50 \pm 0.01$ T) and the samples under a zero-field cooling state. The maximum levitation forces of the samples were achieved at the smallest separation of 0.2 mm. As we can see in this figure, the YBCO bulk superconductor exhibits a maximum levitation force of 38.3 N, while the GdBCO sample presents a maximum levitation force of 29.2 N, which is 23.6% lower than YBCO. However, the GdBCO + CeO₂ sample achieves a maximum levitation force of 54.5 N, which is 42.3% higher than YBCO and 86.6% higher than undoped GdBCO sample. The calculated maximum

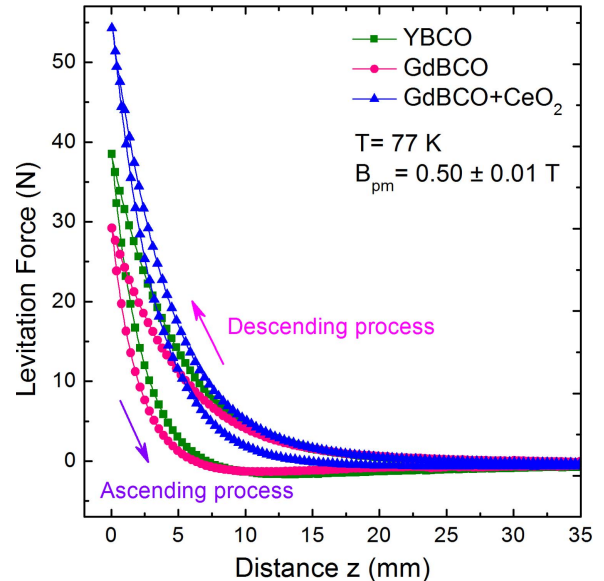


Figure 5. The levitation forces versus distance at 77 K for the single domain YBCO, GdBCO and GdBCO + CeO₂ superconductor bulks.

force density of the GdBCO + CeO₂ sample is above 17.3 N cm⁻², which is a superior performance and even higher than that observed in a Li₂CO₃ doped GdBCO sample under an optimum doping level fabricated by the Gd + O11 TSIG process, which is about 12.3 N cm⁻² (38.5 N for a sample diameter 20 mm) [11]. We can also see from figure 5 that the gap between the descending and ascending curves for the GdBCO + CeO₂ sample is smaller than for the undoped REBCO bulks, which indicates the superior pinning property of the GdBCO bulk with CeO₂ doping. These results prove that, based on the RE + O11

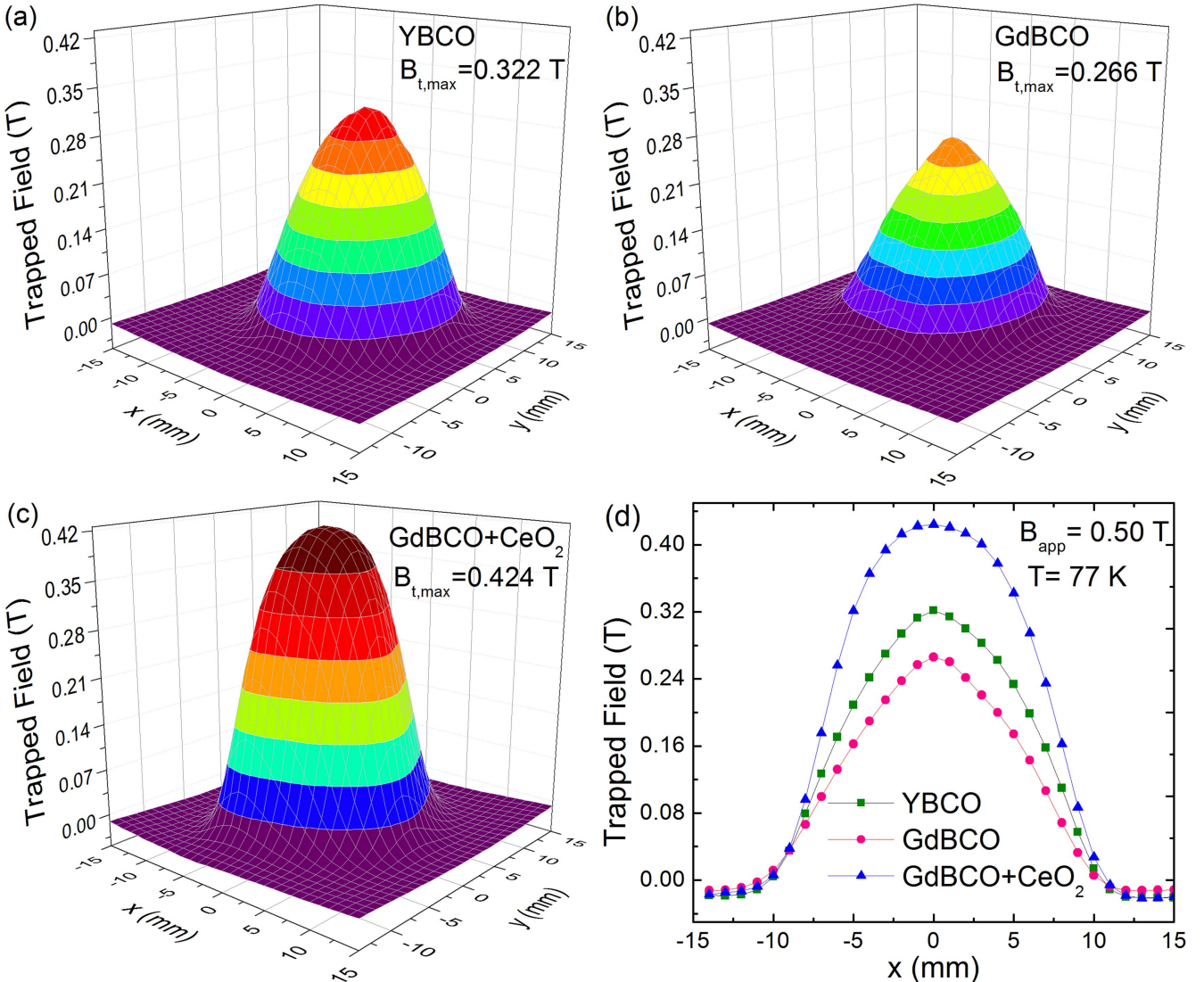


Figure 6. 3D contour maps of the trapped field distributions of the single domain (a) YBCO, (b) GdBCO and (c) GdBCO + CeO₂ superconductor bulks with B_{app} = 0.50 T at 77 K. (d) Trapped fields along the diameters of the YBCO, GdBCO and GdBCO + CeO₂ superconductor bulks.

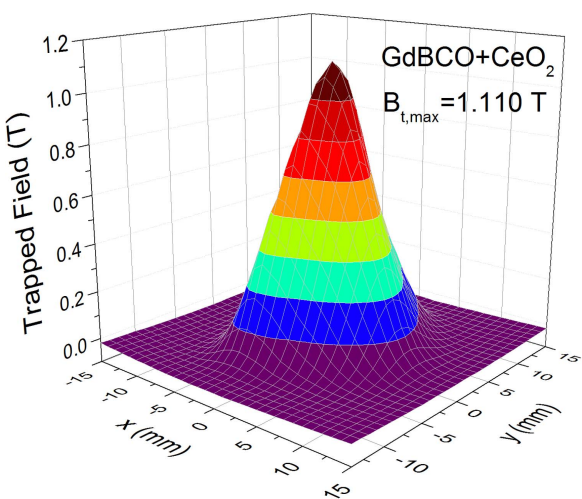


Figure 7. 3D contour map of the trapped field distribution of the single domain GdBCO + CeO₂ superconductor bulks with B_{app} = 1.80 T at 77 K.

TSIG processes, the undoped single domain REBCO bulks fabricated by the novel configurations show a good performance, and more importantly, the GdBCO bulk containing 1 wt% CeO₂ exhibits an excellent levitation force performance.

3.3. Trapped field

The trapped fields were measured using a cryogenic scanning Hall probe after the samples magnetized at an applied field of 0.50 T (B_{app} = 0.50 T) by an electromagnet under a field cooling state at 77 K. Figure 6 shows the 3D contour maps of trapped field distribution and the trapped fields along the diameters of the single domain YBCO, GdBCO and GdBCO + CeO₂ superconductor bulks. It is clear from figure 6 that all these three samples exhibit the single peak in their trapped field distribution profile, which means they are all of a single domain growth in magnetism. The maximum trapped field values observed for undoped YBCO and GdBCO are 0.322 T and 0.266 T, respectively. The GdBCO

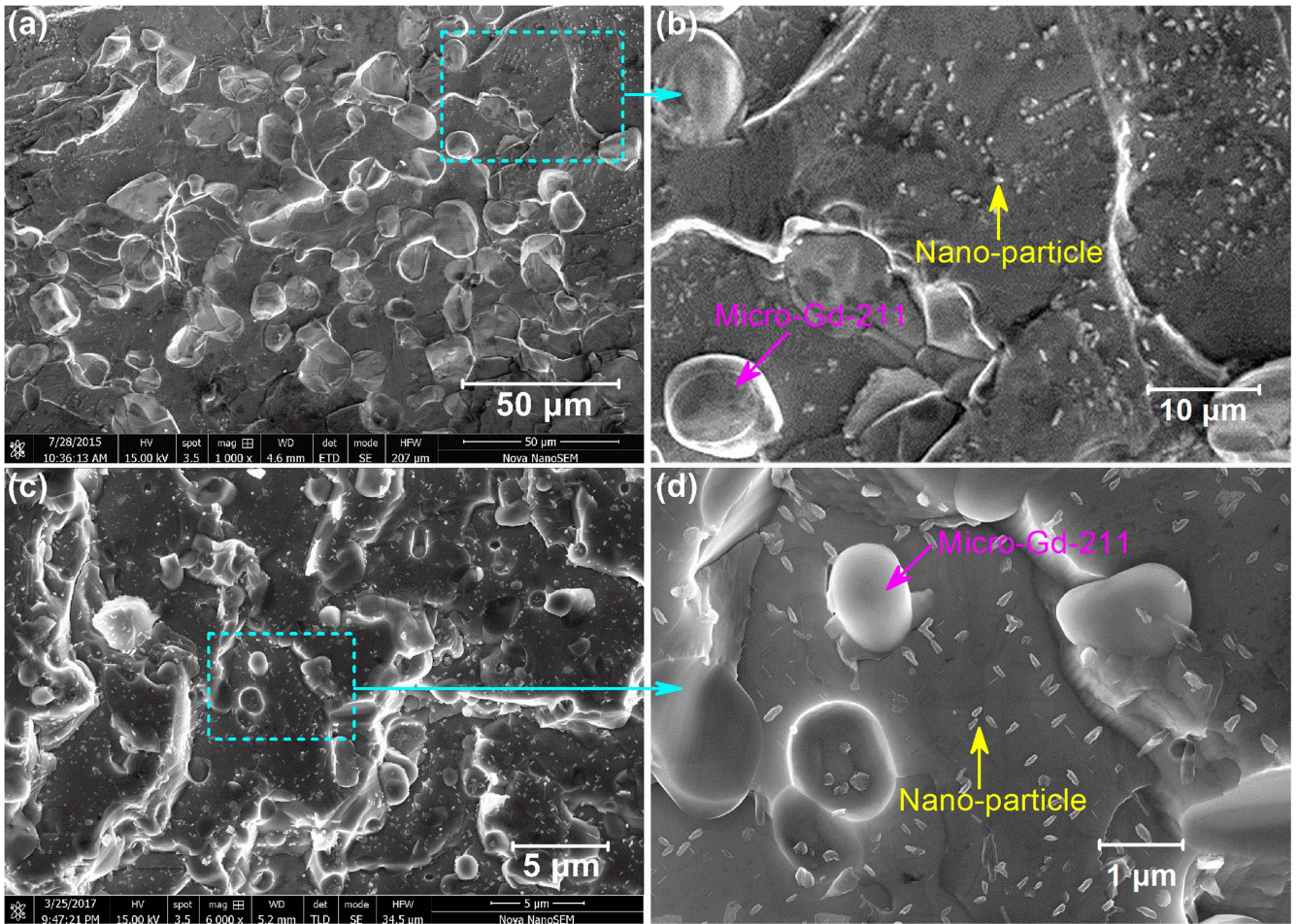


Figure 8. SEM micrographs of a/b planes of the undoped GdBCO and GdBCO + CeO₂ samples. (a), (b) Undoped GdBCO samples, (c), (d) GdBCO + CeO₂ samples.

superconductor grown from SPP powders containing 1 wt% CeO₂ exhibits a maximum trapped field of 0.424 T, which is 31.7% and 59.4% higher than the undoped YBCO and GdBCO superconductors, respectively. These results indicate that, based on the RE + 011 TSIG processes, the undoped single domain REBCO bulks fabricated using the novel configurations have reasonable trapped fields, but the GdBCO bulk superconductor with 1 wt% CeO₂ doping has a better trapped field performance.

Considering the excellent trapped field of the GdBCO + CeO₂ sample magnetized by $B_{app} = 0.50$ T at 77 K, we assumed that the trapped field of the 1 wt% CeO₂ doped GdBCO sample could be enhanced if it is magnetized under a higher magnetic field, so a higher field of $B_{app} = 1.80$ T was used to magnetize this sample at 77 K. The 3D contour map of the trapped field of the single domain GdBCO + CeO₂ sample is shown in figure 7, the maximum trapped field value is 1.110 T, which is 63.2% higher than the trapped field (0.68 T) of the graded-CeO₂ YBCO superconductors with the same diameter [18]. Considering that the GdBCO + CeO₂ sample is only 20 mm in diameter, the trapped field value of 1.110 T is a very good result, which is 20.7% higher than the trapped field (0.92 T) of the graded-CeO₂ YBCO superconductors with a diameter of 31 mm [18].

3.4. Microstructure

In order to make clear why the levitation force (54.5 N) and the trapped field (0.424 T) of the GdBCO + CeO₂ sample are much higher than the levitation force (29.2 N) and the trapped field (0.266 T) of the undoped GdBCO sample, the microstructures of the two samples have been observed using SEM, as shown in figures 8 and 9. Figure 8 shows the SEM micrographs of the a/b planes of the samples, as we can see from these figures, there are many micro-size Gd-211 particles and unknown nano-size particles in the Gd-123 matrix. We can see from figure 8(a) that the size of the micro-Gd-211 particles in the undoped GdBCO sample is mainly in the range of 5–25 μ m, which is much bigger than the micro-Y-211 particles (from 1–5 μ m) in the undoped YBCO sample fabricated by the Y + 011 TSIG process [13]. However, the size of the micro-Gd-211 particles in the GdBCO + CeO₂ sample is just in the range of 1–3 μ m, as shown in figure 8(c), which is much smaller than that in the undoped GdBCO sample. We can also see from figure 8(b) that the size of the nano-particles in the undoped GdBCO sample is mainly in the range of 500 nm to 1 μ m, but the size of nano-particles in GdBCO + CeO₂ sample is about 100–300 nm, which is smaller than that in the undoped GdBCO sample, as shown in

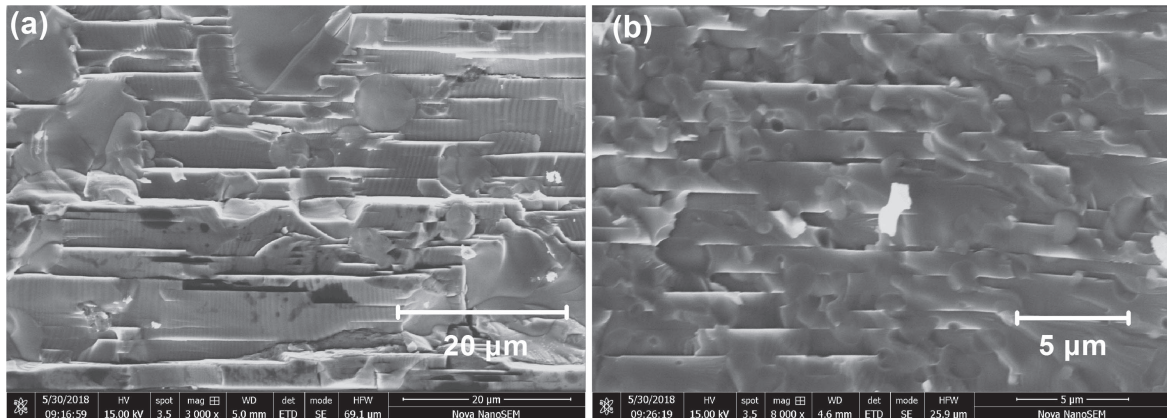


Figure 9. SEM micrographs of the a/c planes of the undoped GdBCO (a) and GdBCO + CeO₂ samples (b).

figure 8(d). More importantly, the distribution of the nanoparticles in the GdBCO + CeO₂ sample is much more homogeneous than that in the undoped GdBCO sample. Figure 9 shows the SEM micrographs of the a/c planes of the samples, as we can see from these figures, the undoped GdBCO and GdBCO + CeO₂ samples have an analogous type of microstructure consisting of a lamellar GdBCO crystal grain and Gd-211 particles, but the thickness of the lamellar GdBCO crystal grain is much different. We can see from figure 9(a) that the thickness of the lamellar GdBCO crystal grain in the undoped GdBCO sample is mainly in the range of 1–6 μm, but its thickness in the GdBCO + CeO₂ sample is just in the range of 0.8–2.2 μm. These indicate that the addition of 1 wt% CeO₂ in the GdBCO sample can greatly refine the size of the micro-Gd-211 particles and nano-particles trapped in the Gd-123 phase matrix and homogenize the distribution of the micro-Gd-211 particles and nano-particles. Compared with the low pinning center density of the GdBCO samples fabricated by the traditional TSIG process, the samples with refined and homogeneous micro-Gd-211 particles and nano-particles can act as effective flux pinning centers to enhance the flux pinning force and physical properties of the samples.

4. Conclusions

Single domain YBCO and GdBCO bulk superconductors with diameter of 20 mm have been fabricated by using the novel configurations, which provide new ways to obtain REBCO superconductors with an easily removable residual liquid phase in the TSIG process. A YBCO bulk superconductor exhibits a higher levitation force and trapped field than an undoped GdBCO in the same conditions. The addition of CeO₂ can greatly refine the size of the micro-Gd-211 particles and nano-particles trapped in the Gd-123 phase matrix, and homogenize their distribution in samples, especially those fabricated by the Gd + 011 TSIG process. The maximum levitation force of 54.5 N (77 K, 0.5 T) and trapped field of 1.110 T (77 K, B_{app} = 1.8 T) were obtained in the GdBCO sample with 1 wt% CeO₂ addition. It is clear from this study that the combination of the novel configurations

and the addition of CeO₂ can not only fabricate high quality single domain REBCO bulk superconductors, but also fabricate near net shape single domain REBCO bulk superconductors without any mechanical processes, which is potentially significant for practical applications of bulk REBCO superconductors.

Acknowledgments

This work was supported by the National Natural Science Foundation in China (No. 51572164, 51342001), the Key-grant Project of the Chinese Ministry of Education (No. 311033), the Research Fund for the Doctoral Program of Higher Education of China (No. 20120202110003), the Key Program of Science and Technology Innovation Team in Shaanxi Province (grant No. 2014KTC-18), and the Fundamental Research Funds for the Central Universities (Nos. 2017CBZ001, GK201505028, GK201305014).

ORCID iDs

Pengtao Yang <https://orcid.org/0000-0001-9397-8734>

References

- [1] Hull J R, Hanany S, Matsumura T, Johnson B and Jones T 2005 *Supercond. Sci. Technol.* **18** S1–5
- [2] Werfel F N, Floegel-Delor U, Rothfeld R, Goebel B, Wip-pich D and Riedel T 2005 *Supercond. Sci. Technol.* **18** S19–23
- [3] Tomita M and Murakami M 2003 *Nature* **421** 517–20
- [4] Durrell J H *et al* 2014 *Supercond. Sci. Technol.* **27** 082001
- [5] Vajda I, Gyore A, Semperger S, Baker A E, Chong E F H, Mumford F J, Meerovich V and Sokolovsky V 2007 *IEEE Trans. Appl. Supercond.* **17** 1887–90
- [6] Oswald B, Best K J, Setzer M, Söll M, Gawalek W, Gutt A, Kovalev L, Krabbes G, Fisher L and Freyhardt H C 2005 *Supercond. Sci. Technol.* **18** S24–9
- [7] Wang J *et al* 2002 *Physica C* **378–381** 809–14
- [8] Umakoshi S, Ikeda Y, Wongtsatanawarid A, Kim C J and Murakami M 2011 *Physica C* **471** 843–5

- [9] Li G Z, Li D J, Deng X Y, Deng J H and Yang W M 2013 *Cryst. Growth Des.* **13** 1246–51
- [10] Yang W M, Chen L P and Wang X J 2016 *Supercond. Sci. Technol.* **29** 024004
- [11] Yang P T, Yang W M, Yakupu A, Su X Q and Zhang L L 2017 *Ceram. Int.* **43** 3010–4
- [12] Guo Y X, Yang W M, Li J W, Guo L P, Chen L P and Li Q 2015 *Cryst. Growth Des.* **15** 1771–5
- [13] Su X Q, Yang W M, Yang P T, Zhang L L and Yakupu A 2017 *J. Alloys Compd.* **692** 95–100
- [14] Kim C, Kim K and Hong G 1994 *Physica C* **232** 163–73
- [15] Kim C, Kim K, Kuk I and Hong G 1997 *Physica C* **281** 244–52
- [16] Muralidhar M, Koblischka M R and Murakami M 2000 *Supercond. Sci. Technol.* **13** 693–7
- [17] Muralidhar M, Jirsa M, Nariki S and Murakami M 2001 *Supercond. Sci. Technol.* **14** 832–8
- [18] Zhai W, Shi Y, Durrell J H, Dennis A R, Zhang Z and Cardwell D A 2015 *Cryst. Growth Des.* **15** 907–14
- [19] Zhao W, Shi Y, Radusovska M, Dennis A R, Durrell J H, Diko P and Cardwell D A 2016 *Supercond. Sci. Technol.* **29** 125002
- [20] Yang W M, Zhi X, Chen S L, Wang M, Ma J and Chao X X 2014 *Physica C* **496** 1–4
- [21] Shi Y H, Dennis A R and Cardwell D A 2015 *Supercond. Sci. Technol.* **28** 035014
- [22] Yang W M, Zhou L, Feng Y, Zhang P X and Zhang C P 2006 *J. Alloys Compd.* **415** 276–9
- [23] Chen S L, Yang W M, Li J W, Yuan X C, Ma J and Wang M 2014 *Physica C* **496** 39–43